

Cas21 controls higher-order nuclear organization in rod photoreceptors

Pierre Mattar^{a,1,2}, Milanka Stevanovic^{a,b}, Ivana Nad^c, and Michel Cayouette^{a,b,d,e,1}

^aCellular Neurobiology Research Unit, Institut de Recherches Cliniques de Montréal, Montréal, QC H2W 1R7, Canada; ^bDepartment of Anatomy and Cell Biology, McGill University, Montréal, QC H3A 0G4, Canada; ^cDepartment of Cell and Molecular Medicine, University of Ottawa, Ottawa, ON K1H 8M5, Canada; ^dDivision of Experimental Medicine, McGill University, Montréal, QC H3A 0G4, Canada; and ^eDepartment of Medicine, Université de Montréal, Montréal, QC H3T 1J4, Canada

Edited by Chris Q. Doe, HHMI and University of Oregon, Eugene, OR, and approved July 11, 2018 (received for review February 19, 2018)

Genome organization plays a fundamental role in the gene-expression programs of numerous cell types, but determinants of higher-order genome organization are poorly understood. In the developing mouse retina, rod photoreceptors represent a good model to study this question. They undergo a process called “chromatin inversion” during differentiation, in which, as opposed to classic nuclear organization, heterochromatin becomes localized to the center of the nucleus and euchromatin is restricted to the periphery. While previous studies showed that the lamin B receptor participates in this process, the molecular mechanisms regulating lamina function during differentiation remain elusive. Here, using conditional genetics, we show that the zinc finger transcription factor Cas21 is required to establish and maintain the inverted chromatin organization of rod photoreceptors and to safeguard their gene-expression profile and long-term survival. At the mechanistic level, we show that Cas21 interacts with the polycomb repressor complex in a splice variant-specific manner and that both are required to suppress the expression of the nuclear envelope intermediate filament lamin A/C in rods. Lamin A is in turn sufficient to regulate heterochromatin organization and nuclear position. Furthermore, we show that Cas21 is sufficient to expand and centralize the heterochromatin of fibroblasts, suggesting a general role for Cas21 in nuclear organization. Together, these data support a model in which Cas21 cooperates with polycomb to control rod genome organization, in part by silencing lamin A/C.

chromatin | photoreceptors | mouse | retina | neurodegeneration

The mammalian nucleus must compartmentalize a genome measuring about 2 m in length into a structure that is less than 600 μm^3 in volume (1, 2). To maintain genome organization, chromatin is packaged into functional domains organized according to a variety of mechanisms. At the highest level, the genome is partitioned into active A and inactive B compartments that exhibit segregated higher-order looping interactions that can be further subdivided (3, 4). Topologically associated domains (TADs), similarly divide chromosomes into megabase-scale units with internally restricted chromosome folding (5). TADs are also highly stable among different cell types. Structures such as the nuclear lamina, nucleolus, and nuclear pores additionally associate with chromatin and modify its activity. Epigenetic modifications also partition the genome into a hierarchy of euchromatin and heterochromatin types with differing levels of accessibility and compaction. While it has long been known that these factors cooperate to control the genome, it remains challenging to dissect how cells modify this organization and, in turn, how global changes relate to different transcriptomic states and cellular functions.

The developing mouse retina provides an advantageous model system in which to address these issues. Upon differentiation, rod photoreceptors undergo a process called “chromatin inversion” in which heterochromatin becomes localized to the center of the nucleus and the euchromatin to the periphery (6, 7), which is the opposite of the classic nuclear organization observed in most eukaryotic cells. Chromatin inversion was proposed as an adaptation to nocturnal vision that reduces light

scattering in the retina (7). While previous studies have provided a descriptive framework for understanding rod genome organization, determinants of this organization remain largely elusive, with only the lamin B receptor (Lbr) identified so far (8).

Here, we report that Cas21 is a determinant of rod photoreceptor nuclear organization. Cas21 is a zinc finger transcription factor required for both heart and vascular development, and its germline inactivation causes embryonic lethality (9–11). Cas21 is orthologous to the *Drosophila melanogaster* gene *castor* (12–14). In flies, *castor* participates in shaping the lineages of most neuroblasts (stem cells) of the central nervous system (15–19) and appears to act exclusively as a transcriptional repressor (17, 20). *Castor* is also widely expressed in postmitotic neurons in the fly, but its role in neurons has not been established.

We have previously shown that, similar to *castor*, Cas21 participates in controlling the temporal output of retinal progenitor cells in the mouse (21). Cas21 expression in retinal progenitor cells increases as development proceeds, and we found that Cas21 has a role in promoting rod production from these progenitors. Intriguingly, Cas21 remains expressed in rods and cones upon differentiation, suggesting that it might have a functional role in photoreceptors. Accordingly, we found that genetic

Significance

Eukaryotic cells depend on precise genome organization within the nucleus to maintain an appropriate gene-expression profile. Critical to this process is the packaging of functional domains of open and closed chromatin to specific regions of the nucleus, but how this is regulated remains unclear. In this study, we show that the zinc finger protein Cas21 regulates higher-order nuclear organization of rod photoreceptors in the mouse retina by repressing nuclear lamina function, which leads to central localization of heterochromatin. Loss of Cas21 in rods leads to an abnormal transcriptional profile followed by degeneration. These results identify Cas21 as a regulator of higher-order genome organization.

Author contributions: P.M. and M.C. designed research; P.M., M.S., and I.N. performed research; P.M., M.S., and M.C. analyzed data; and P.M., M.S., and M.C. wrote the paper.

The authors declare no conflict of interest.

This article is a PNAS Direct Submission.

This open access article is distributed under Creative Commons Attribution-NonCommercial-NoDerivatives License 4.0 (CC BY-NC-ND).

Data deposition: The data reported in this paper have been deposited in the Gene Expression Omnibus (GEO) database, <https://www.ncbi.nlm.nih.gov/geo> (accession no. GSE115778).

¹To whom correspondence may be addressed. Email: pmattar@ohri.ca or Michel.Cayouette@ircm.qc.ca.

²Present addresses: Ottawa Health Research Institute, Ottawa, ON K1H 8L6, Canada; and Department of Cell and Molecular Medicine, University of Ottawa, Ottawa, ON K1H 8M5, Canada.

This article contains supporting information online at www.pnas.org/lookup/suppl/doi:10.1073/pnas.1803069115/-DCSupplemental.

Published online August 2, 2018.

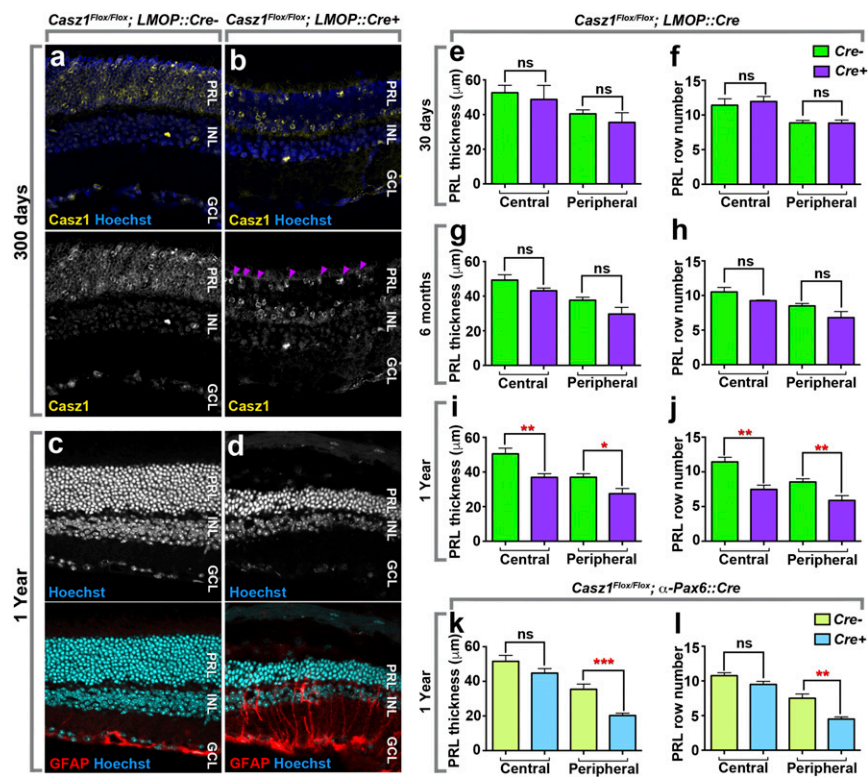


Fig. 2. Genetic ablation of *Cas21* in rod photoreceptors leads to degeneration. (A and B) *Cas21* immunohistochemical staining in adult *Cas21^{Flox/Flox}* retinas (A) or *Cas21 Rod-CKO* (*Cas21^{Flox/Flox}; LMOP::Cre⁺*) retinas (B). Loss of *Cas21* protein is observed in most of the cells within the photoreceptor layer (PRL). However, cone photoreceptors retain protein expression as predicted (arrowheads). (C and D) Retinal sections from 1-y-old *Cas21 Rod-CKO* mice. Photoreceptor degeneration is shown by the thinning of the photoreceptor layer and obvious gliosis detected by the up-regulation of GFAP. (Magnification: A–D, 400×.) (E–L) Quantification of photoreceptor degeneration in *Cas21 Rod-CKO* or progenitor *CKO* (*Cas21^{Flox/Flox}; αPax6::Cre⁺*) mice. (E–L) Loss of rod cells was measured by quantitating the thickness of the photoreceptor layer (E, G, I, and K) or by counting the number of rods found in columns spanning the apico-basal axis (F, H, J, and L), using defined regions of the central or peripheral retina (E–J). In *Cas21 Rod-CKO* mice, loss of rod cells was not detectable at 30 d or 6 mo but reached statistical significance at 1 y. As reported previously (21), rod degeneration was also observed in aged *Cas21^{Flox/Flox}; αPax6::Cre-CKO* mice (K and L), in which Cre is expressed specifically in the peripheral retina during retinal development. ns, not significant. **P* < 0.05, ***P* < 0.01, ****P* < 0.001. The full statistics are presented in *SI Appendix, Table S1*.

Cas21 isoforms could not be detected from retinal lysates using conventional methodology (data not shown), echoing difficulties previously encountered with immunohistochemistry (21). To assist the retrieval of *Cas21* protein, we therefore

performed cross-linking–assisted immunoprecipitation using the rapid immunoprecipitation mass spectrometry of endogenous proteins (RIME) proteomic workflow (33). Using this approach, Rnf2 was very robustly immunoprecipitated from retinal nuclear

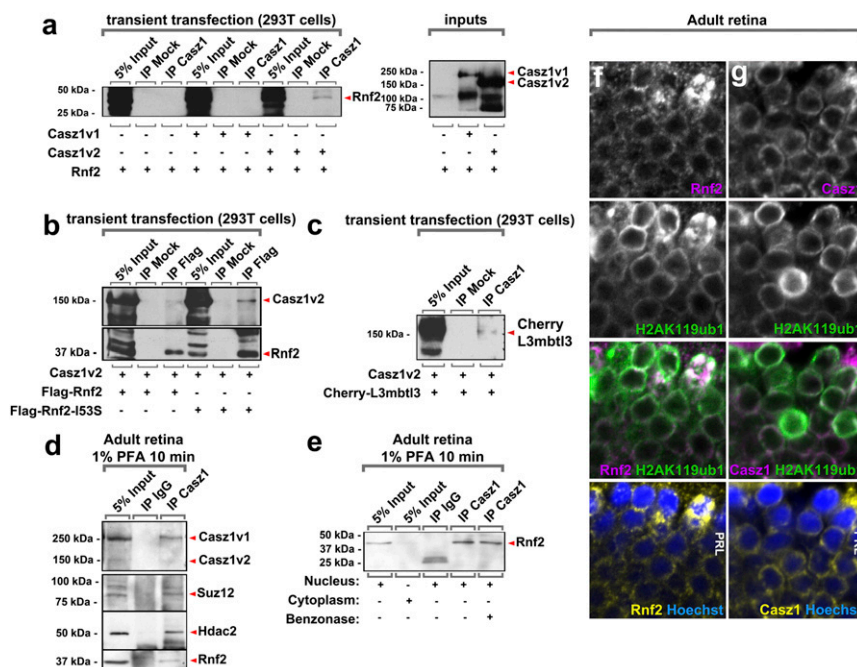


Fig. 3. *Cas21* interacts with the polycomb repressor complex in rod photoreceptors. (A) *Cas21* immunoprecipitations (IP) from cotransfected 293 cells contain Rnf2. Only the *Cas21v2* immunoprecipitation contains Rnf2 protein. (B) Reverse immunoprecipitation of *Cas21v2* using an antibody recognizing Rnf2. (C) *Cas21* immunoprecipitations from cotransfected 293 cells contain L3mbtl3. (D) *Cas21* immunoprecipitations generated via the RIME workflow (33) from adult retinal nuclear extracts contain the polycomb proteins Suz12 and Rnf2. (E) The interaction between *Cas21* and Rnf2 is maintained when genomic DNA is degraded with benzonase. (F and G) Colocalization of *Cas21*, Rnf2, and the polycomb mark H2AK119ub1 in adult photoreceptors. (Magnification: F and G, 1,890×.)

extracts using Casz1 antibodies (Fig. 3 *D* and *E*). Suz12, another polycomb protein associated with polycomb repressive complex 2 (PRC2), was also immunoprecipitated by Casz1 (Fig. 3*D*). The Mi2/Nurd effector protein Hdac2 had been repeatedly shown to interact with Casz1-containing protein complexes (32, 34), and we accordingly observed that retinal Casz1 immunoprecipitated Hdac2 (Fig. 3*D*). Additionally, the Casz1/Rnf2 interaction was not altered when DNA was degraded using benzonase, suggesting that the proteins were not tethered together by DNA (Fig. 3*E*). Finally, we examined the expression of Rnf2 and its target histone modification H2AK119ub1 in adult retinas using antibodies previously validated on mutant cells (35, 36). We found that both Rnf2 and H2AK119ub1 colocalized with Casz1 in the nuclear periphery of rods (Fig. 3 *F* and *G*). We conclude that the Casz1v2 isoform forms complexes with transcriptional corepressors, including polycomb.

Cas1 Regulates Nuclear Lamina Function. To examine the functional effects of Cas1 on rod photoreceptors, we first overexpressed both *Cas1v1* and *Cas1v2* splice forms in rods by electroporating postnatal retinal explants with the pCIG2 expression vector, which allows us to mark all transfected cells simultaneously via an IRES2-EGFP cassette. Explants were allowed to develop for 2 wk, and the resultant rods were examined in retinal sections. We noted striking effects of *Cas1v2* on rods, with transfected cells exhibiting a clear bias to localize their nuclei to the basal side of the photoreceptor layer, adjacent to the outer plexiform layer (Fig. 4 *G–I*, *S*, and *T* and *SI Appendix*, Table S2). Opposite effects were observed when RNAi was used to knock down Cas1 or polycomb proteins such as Ring1a or Rnf2, where transfected cell somas migrated to the apical side of the layer (Fig. 4 *J–O*, *S*, and *T*). Moreover, the effect of *Cas1v2* overexpression was blocked by knocking down Rnf2, indicating that *Cas1v2* depends on Rnf2 to control rod nuclear position (Fig. 4 *P–T*).

It is well known that the apico-basal nuclear position in the photoreceptor layer is regulated by the nuclear lamina. Basal migration of photoreceptor nuclei is associated with disruption of lamina components such as laminB2, Sun1/2, Syne2, and associated dynein motors (37–42). We thus predicted that Cas1 might affect the expression of lamina proteins. As expected, whereas rods transfected with an empty RNAi control vector exhibited no lamin A/C expression and no alteration in Lbr levels (Fig. 5*A* and *SI Appendix*, Fig. S24), rods transfected with shRNA constructs targeting Ring1, Rnf2, or Cas1 up-regulated lamin A/C (Fig. 5*B* and *C* and *SI Appendix*, Fig. S2*B* and *C*). Importantly, no cones were targeted by postnatal transfections, in accordance with previous reports, due to the exclusively embryonic temporal window for cone generation (*SI Appendix*, Fig. S34) (43, 44).

To confirm that the observed up-regulation of lamin A/C was due to specific knockdown of Ring1 or Rnf2 rather than off-target effects, we overexpressed Mym1, which deubiquitinates H2AK119 in opposition to Ring1 and Rnf2 (45). Accordingly, Mym1 likewise led to the up-regulation of lamin A/C expression (*SI Appendix*, Fig. S2*D*). We also confirmed that the apical nuclear position phenotype triggered by shRnf2 could be rescued by coexpressing it with a human Rnf2 construct that was mismatched with the shRNA hairpin due to evolutionary divergence (*SI Appendix*, Fig. S4).

We next examined *Cas1*-cKO rods generated using the retinal progenitor α -Pax6::Cre driver (46). Within the central retina, where the Cre driver is generally not expressed during development, we found that, as previously reported (8, 47), lamin A/C expression was confined to cones, which localize apically in the photoreceptor layer (Fig. 5*D* and *SI Appendix*, Fig. S5). Conversely, many more photoreceptors expressed lamin A/C in the peripheral retina (Fig. 5*E* and *F*), where the Cre driver is most highly expressed during development (46). Many of these cells were very clearly rods, based on their nuclear morphology and

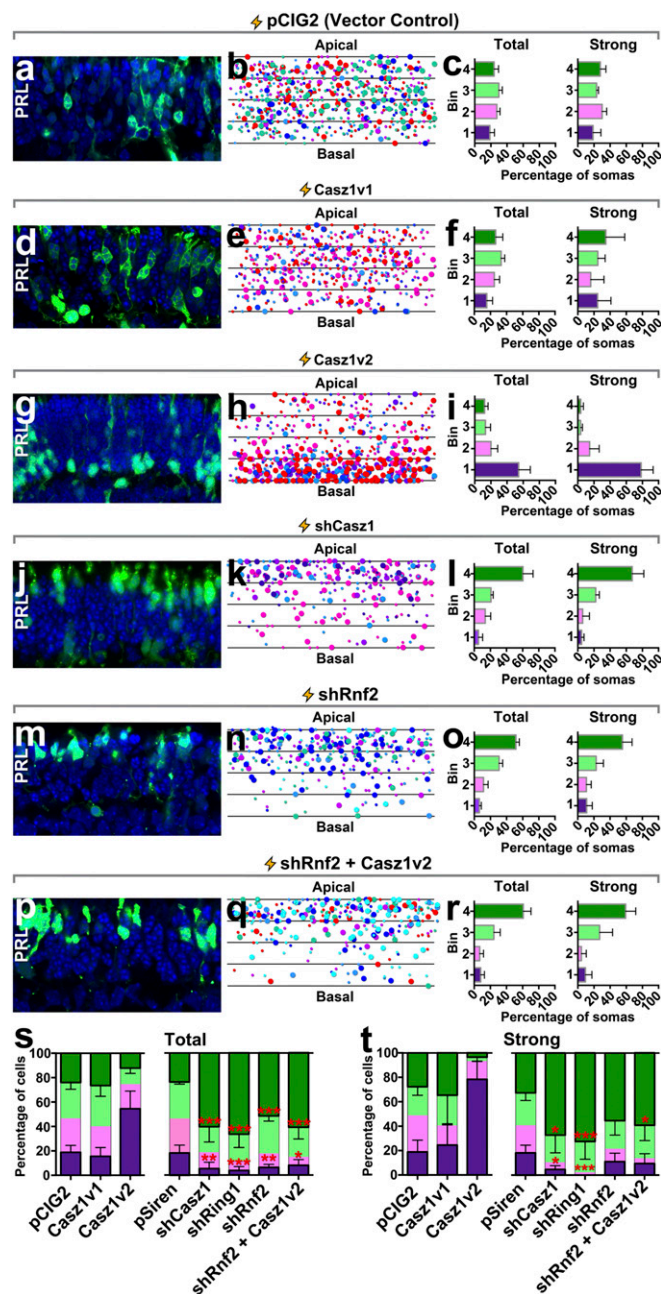


Fig. 4. Cas1 and polycomb control rod nuclear position. P0/P1 retinal explants were transfected with the indicated constructs and cultured for 2 wk to allow rods to be produced. Explants were then harvested, sectioned, and imaged (*A*, *D*, *G*, *J*, *M*, and *P*; magnification: 630 \times). Each photoreceptor layer was divided into four equal-sized bins, and the centroid position of each rod nucleus was plotted (*B*, *E*, *H*, *K*, *N*, and *Q*). Rods were considered strongly transfected (strong) if they exhibited pixel saturation under the imaging conditions. These cells are indicated by larger circles in the plots; weaker transfected cells are indicated by smaller circles. Colors correspond to different experimental replicates. The proportion of total or strongly transfected rod nuclei within each of the four bins was then obtained (*C*, *F*, *I*, *L*, *O*, and *R*). (*S* and *T*) Comparison of total (*S*) or strongly transfected (*T*) rods. The indicated statistical inferences reflect multivariate comparisons via one-way ANOVA and Tukey's post hoc test for a given bin between all other experimental treatments. Bins 2 and 3 were not analyzed statistically. pCIG2, Casz1v1, and Casz1v2 were not included in the ANOVA and are reproduced here only for visual comparison (Fig. 7). * $P < 0.05$; ** $P < 0.01$; *** $P < 0.001$, significantly different versus control.

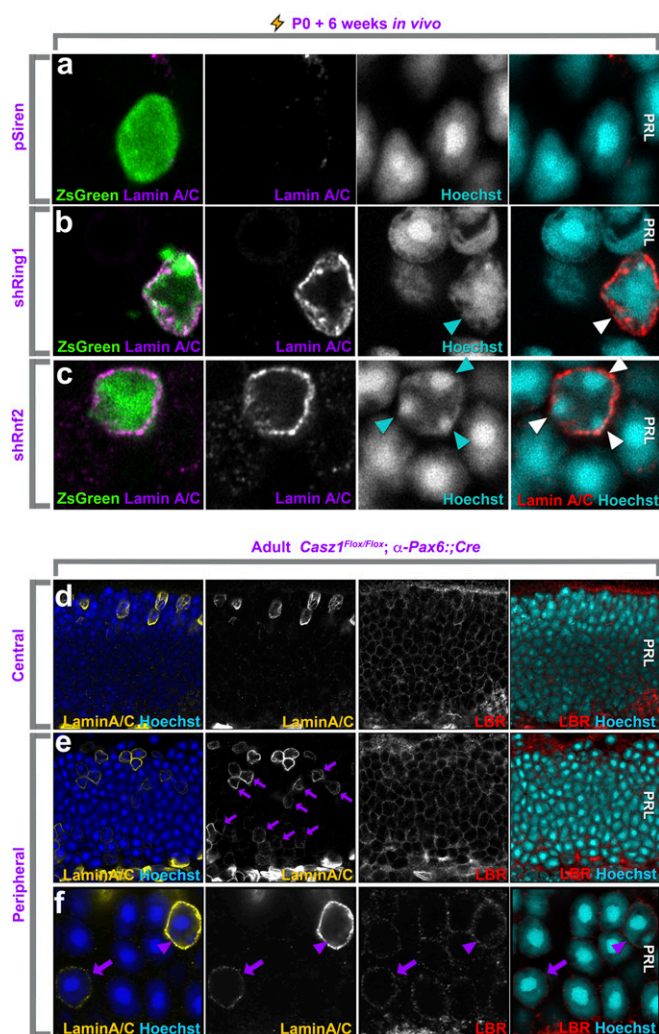


Fig. 5. Up-regulation of lamin A/C is associated with polycomb or *Cas21* loss of function. (A–C) Airyscan confocal images of retinal explants transfected with control constructs or shRNA constructs targeting Ring1 or Rnf2. Arrowheads mark heterochromatin contacting the nuclear lamina specifically in transfected cells. (D–F) Airyscan confocal analysis of lamin A/C or Lbr expression in *Cas21*-cKO retinas generated using the α -Pax6::Cre driver. The central retina does not express Cre during development and serves as an internal control (D). (E and F) Arrows mark lamin A/C up-regulation in basally located rod nuclei. The arrowhead in F marks an apically localized cone nucleus, which normally expresses lamin A/C. (Magnification: A–C, 6,300 \times ; D and E, 945 \times ; F, 3,150 \times .)

more basal nuclear position (Fig. 5 E and F). Lamin A/C⁺ rods also lacked expression of cone markers (SI Appendix, Fig. S3 B and C). Thus, loss of either *Cas21* or its polycomb cofactors results in the ectopic up-regulation of lamin A/C.

To determine whether lamin A/C was sufficient to explain the observed nuclear position effects, we overexpressed N-terminal GFP-fusion proteins encoding lamin A (prelamin A) and progerin, a lamin variant harboring a C-terminal truncation, but found that these constructs had no effect on nuclear position (Fig. 6 A–N and SI Appendix, Table S3). We additionally overexpressed a construct encoding an untagged version of lamin A in photoreceptors using explant electroporation. Surprisingly, we found that untagged lamin A was sufficient to force localization of photoreceptor soma to the apical side of the neural retina (Fig. 6 J–N). These results suggested that the N-terminal GFP tag was function blocking. Both tagged and untagged lamin

A proteins localized correctly to the nuclear periphery, although the GFP-lamin A construct generated protein inclusions that were not apparent in cells transfected with the untagged version (SI Appendix, Fig. S6). We conclude that lamin A is sufficient to promote apical migration of photoreceptor nuclei.

In addition to nuclear position, the lamina also regulates heterochromatin tethering (8). In the absence of functional lamina tethers such as Lbr, cells undergo chromatin inversion in which chromocenters relocate to the center of the nucleus instead of maintaining their default localization at the nuclear envelope (7, 8). Previous work using transgenic mice had shown that lamin C was not sufficient to affect chromatin inversion, but the role of lamin A was not explored.

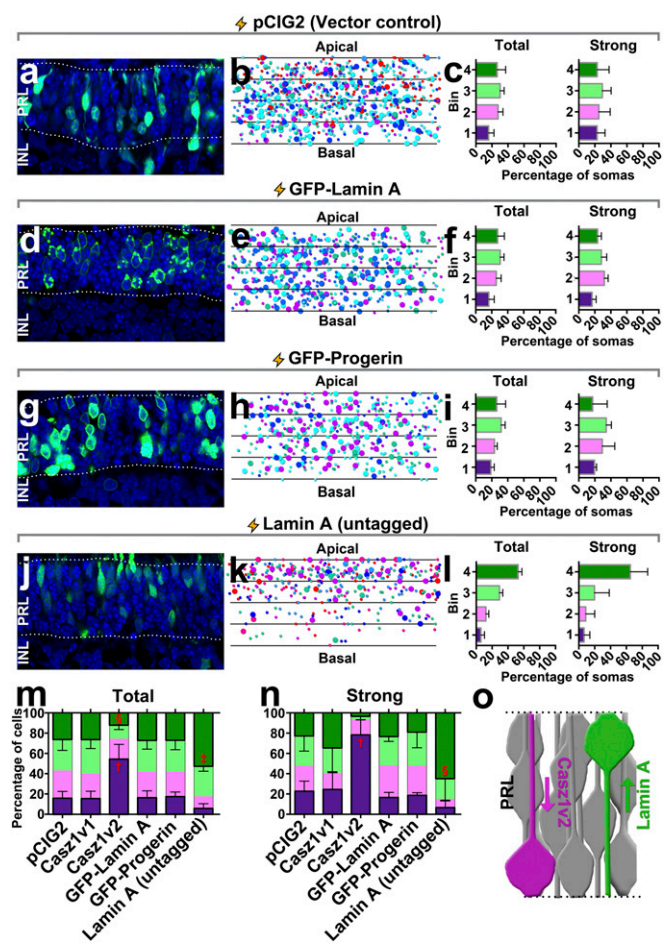


Fig. 6. Lamin A controls rod nuclear position. (A–L) P0 Retinal explants were transfected with the indicated constructs and cultured for 2 wk to allow rods to be produced. Explants were then harvested, sectioned, and imaged. Note that the EGFP signal in D and G is fused directly to lamin A, whereas the EGFP signal in A and J is coexpressed from an IRES cassette. Each photoreceptor layer was divided into four equal-sized bins, and the centroid position of each rod nucleus was plotted as detailed in Fig. 4. (Magnification: A, D, G, and J, 630 \times .) (M and N) Comparison of total (M) or strongly transfected (N) rods. The indicated statistical inferences reflect multivariate comparisons via one-way ANOVA and Tukey's post hoc test for a given bin versus all other experimental treatments. Bins 2 and 3 were not analyzed statistically. [†] $P < 0.0001$, significantly different from all other treatments; [‡] $P < 0.001$, significantly different from all other treatments; [§] $P < 0.05$, significantly different from all other treatments. (O) Model for the effects of *Cas21* and lamin A on nuclear position. *Cas21v2* opposes the function of the nuclear lamina, leading to basal localization of the rod nucleus. Lamin A promotes apical nuclear localization and is dominant over *Cas21v2*.

To assess the effects of lamin A on chromatin inversion, we electroporated retinas of P0 mice in vivo and harvested the tissues 6 wk later, when rod chromatin inversion is complete. Whereas control or GFP-Lamin A overexpression had little to no effect on chromatin inversion (Fig. 7A–F), a striking blockade of chromatin inversion was observed in rods overexpressing untagged lamin A (Fig. 7C–F). While the proportion of the nucleus occupied by heterochromatin was reduced by only ~20% (Fig. 7D and *SI Appendix, Table S4*), both the number of chromocenters and the proportion of chromocenters contacting the nuclear lamina were significantly increased compared with control or GFP-lamin A (Fig. 7E and F). These data show that lamin A is a powerful suppressor of chromatin inversion.

The strong effects elicited by lamin A overexpression led us to revisit *Cas21*-cKO rods, which up-regulate lamin A/C (Fig. 5E and F and *SI Appendix, Fig. S3B and C*). While increased chromocenter/lamina contacts had been observed in *Cas21*/polycomb RNAi electroporations (Fig. 5B and C and *SI Appendix, Figs. S2 and S3A*), defects in *Cas21*-mutant rods were not easy to detect at adult stages in vivo using confocal or even Airyscan super-resolution microscopy. The only discernable effect was that some mutant rod nuclei appeared to be slightly more disordered than in controls. However, this defect was much more apparent when rods were visualized with transmission electron microscopy (TEM). We examined *Cas21*-cKO rods from the peripheral retinas of *Cas21^{Flox/Flox}; α-Pax6::Cre*-cKO animals, where Cre is expressed (46), and compared these with rods from the peripheral retinas of Cre⁻ animals. We found that *Cas21*-cKO rods exhibited highly eccentric heterochromatin in comparison with littermate controls (Fig. 7G and H). This manifested as a significant reduction

in the overall proportion of the nucleus occupied by heterochromatin (Fig. 7I and *SI Appendix, Table S4*). Chromocenter/lamina contacts were also increased by approximately twofold in the *Cas21*-KO animals (Fig. 7J and *SI Appendix, Table S4*). Taken together, these results indicate that *Cas21*/polycomb function is required for lamin A/C repression in rods, thereby ensuring normal nuclear positioning and chromatin inversion.

Cas21 Is Sufficient to Induce Aspects of Photoreceptor Nuclear Organization in Fibroblasts. We next investigated whether *Cas21* might contribute directly to chromatin inversion. We first mis-expressed control, *Cas21v1*, or *Cas21v2* in immature rods via explant electroporation at P0 and studied nuclear organization at P14, when all rods have been born but their chromatin inversion is not yet completed. While control and *Cas21v1* transfections had no effect on rod nuclei organization, *Cas21v2* dramatically accelerated chromatin inversion (Fig. 8A–C). Next, we wondered whether *Cas21* would be capable of reorganizing heterochromatin in nonphotoreceptor cells. We analyzed progenitor cells, which constitute the majority of transfected cells, 3 d after electroporation at P0. Progenitors overexpressing *Cas21v2* exhibited centralized and enlarged chromocenters similar to those found in mature rods, whereas control transfections had no effect (Fig. 8D and E). To determine whether these large central chromocenters represented the merging of preexisting heterochromatin or instead reflected de novo production, we performed quantitative microscopy. We found that progenitors overexpressing *Cas21v2* had a decreased mean number of chromocenters per nucleus and a significantly larger nuclear area than control cells (Fig. 8F and G and *SI Appendix, Table S5*).

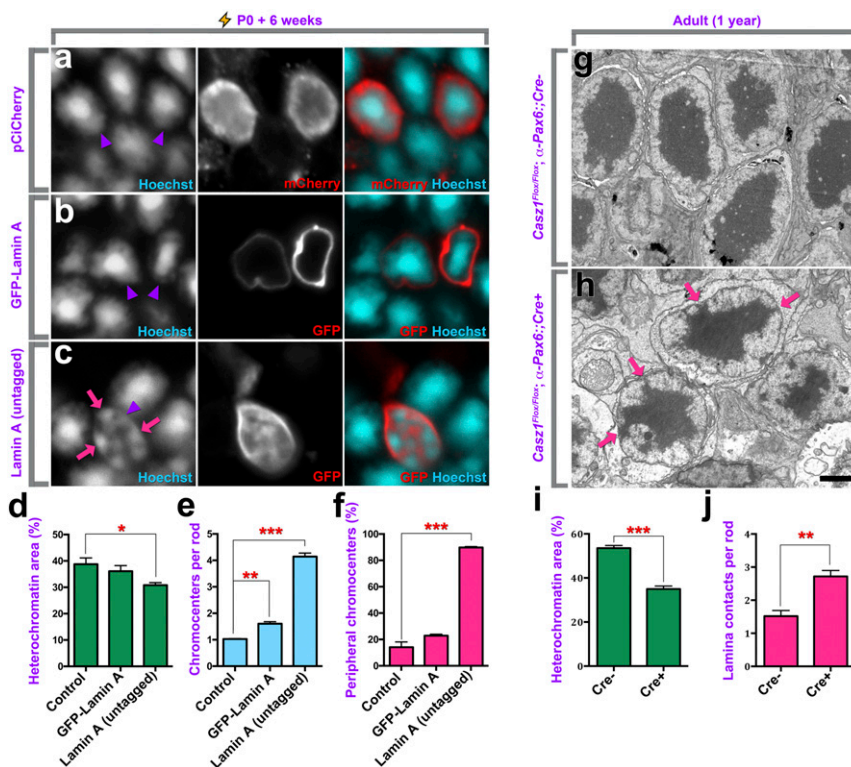


Fig. 7. Lamin A/C is sufficient to block the inversion of rod nuclear architecture. (A–C) Retinas were transfected in vivo at P0, and rods were allowed to differentiate and mature over 6 wk. Retinas were then harvested, and nuclei were visualized via Hoechst staining. Arrowheads mark transfected cells. Note that GFP in B is fused directly to lamin A, whereas the mCherry/GFP signal in A and C is coexpressed from an IRES cassette. (Magnification: A–C, 1,890×.) (D–F) Quantitation of heterochromatin area (D), the number of chromocenters present per rod nucleus (E), and the percentage of chromocenters contacting the nuclear lamina (F). (G and H) Transmission electron micrographs of 1-y-old *Cas21*-cKO rods. Arrows mark aberrant lamina/heterochromatin contacts. (Scale bar, 2 μm.) (I and J) Quantitation of the percentage of the nuclear area occupied by heterochromatin (I) and the number of lamina/heterochromatin contacts per nucleus (J). **P* < 0.05, ***P* < 0.01, ****P* < 0.001, significantly different versus control; *n* = 3.

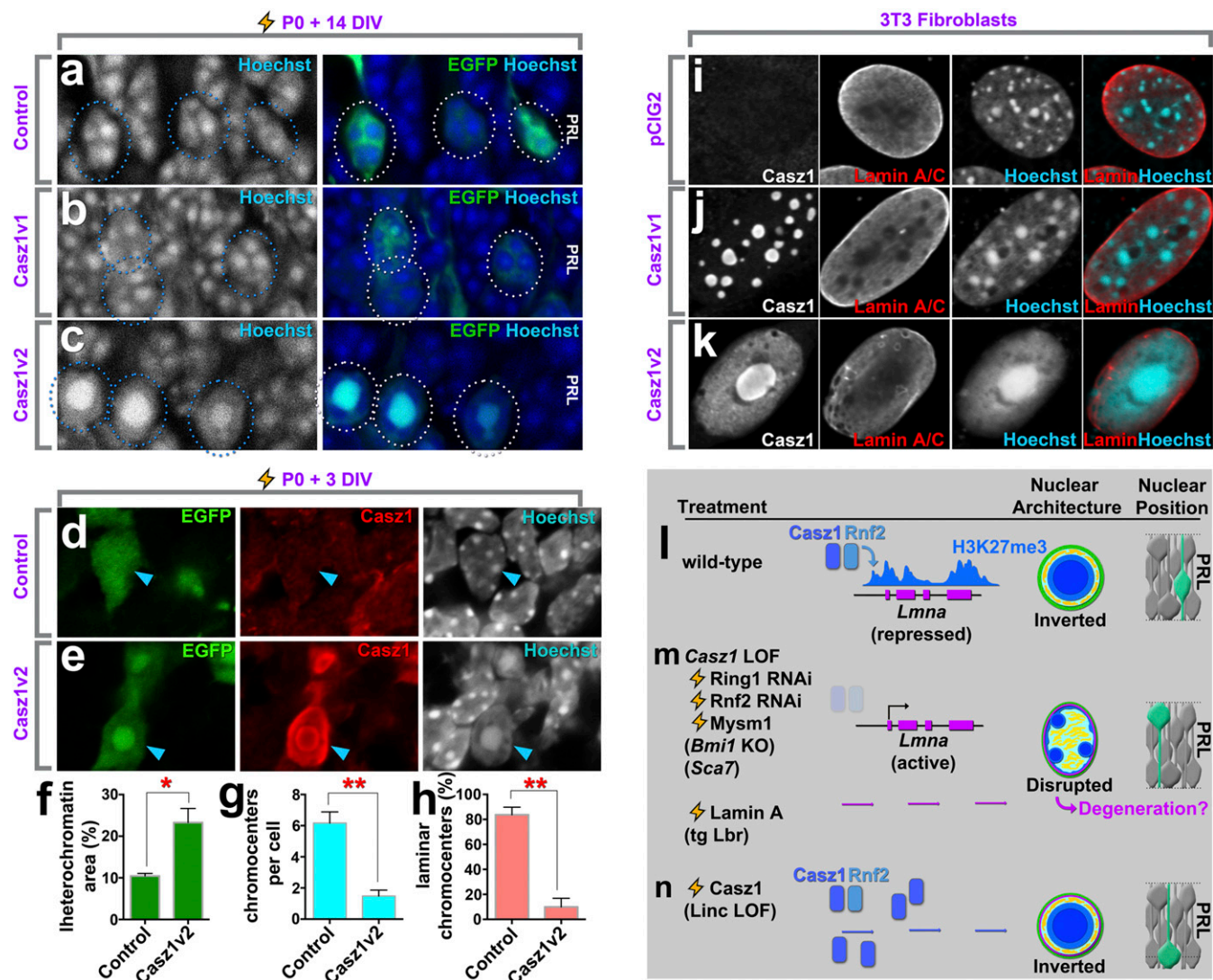


Fig. 8. Casz1 is sufficient for aspects of inverted nuclear organization. Retinal explants were transfected at P0 and cultured for 14 d (A–C) or 3 d (D and E) in vitro with the indicated constructs. Transfected cells were identified by EGFP expression and analyzed for the expression of Casz1. DNA was stained with Hoechst dye. There is little endogenous Casz1 expression in retinal progenitors at ~P4, as we previously reported (21). (F–H) Hoechst staining in transfected cells was quantitatively analyzed for the percentage of the nuclear area occupied by chromocenters (F), the average number of chromocenters per nucleus (G), and the percentage of chromocenters contacting the nuclear margin (H). * $P < 0.05$; ** $P < 0.001$; $n = 3$ independent experiments. (I–K) 3T3 fibroblasts were transfected with the indicated constructs and harvested after 72 h. Cells were subjected to immunocytochemistry for Casz1 and lamin A/C, and nuclei were visualized Hoechst staining. (L–N) Summary of data and working model. (Magnification: A–E and I–K, 1890 \times .) (L) In rods, the *Lmna* gene is coated by the repressive polycomb mark H3K27me3 and is transcriptionally silent (SI Appendix, Fig. S4) (66, 67). Casz1 interacts with the polycomb protein Rnf2 and contributes to *Lmna* repression and thereby chromatin inversion. Nuclear position within the photoreceptor layer is randomized. (M) Casz1 or polycomb cKO or RNAi leads to the up-regulation of lamin A/C expression. Disruption of rod nuclear organization and degeneration also has been reported in mutants for the polycomb gene *Bmi1* and for *Sca7* (61, 73), although lamin A/C up-regulation has been reported only for the latter (8). Reintroduction of heterochromatic tethers such as lamin A or Lbr (8) disrupts the inverted nuclear architecture of rods. In the photoreceptor layer, rod nuclei relocate to the apical side. (N) Casz1 overexpression is sufficient to reorganize the nuclei of heterologous cells even in the presence of lamin A/C. In the photoreceptor layer, rod nuclei localize to the basal side, although lamin A/C is not expressed in rods.

Finally, the percentage of chromocenters touching the nuclear periphery was significantly reduced in cells transfected with Casz1v2 compared with controls (Fig. 8H).

To determine whether Casz1 could reorganize chromatin in nonretinal cells, we overexpressed Casz1 constructs in NIH 3T3 fibroblasts. Overexpression of control or Casz1v1 constructs had little effect on nuclear organization, whereas Casz1v2 transfection led to an aggregation and expansion of chromocenters (Fig. 8 I–K). A proportion of cells exhibited nuclei that strikingly resembled those of mature rod nuclei, with a single chromocenter in the middle of the nuclei. In these cells,

euchromatin became redistributed to the nuclear periphery, although euchromatic marks often remained depleted at the lamina (SI Appendix, Fig. S7). As lamin A/C is highly expressed in fibroblasts, we examined cells transfected with control or Casz1v2 constructs for the expression of lamin A/C to ask whether nuclear reorganization correlated with effects on lamin A/C levels. We found that lamin A/C remained expressed in NIH 3T3 fibroblasts (Fig. 8K). We surmise that while Casz1 is required to silence lamin A/C expression in the retina, Casz1v2 is additionally sufficient to oppose lamina function independently of lamin A/C or Lbr transcriptional repression.

Discussion

Photoreceptor cells are among the most metabolically active cells in the body (48). Probably for this reason, rods and cones are highly sensitive to transcriptomic perturbations. Deficiency in the transcription factors required for activating the rod gene-expression program, such as *Crx*, *Mef2c/d*, *Neurod1*, and *Otx2*, is associated with photoreceptor cell death and retinal degenerative diseases such as retinitis pigmentosa and cone-rod dystrophy (49–54). Reduction of rod gene expression is associated with cell death in many experimental models, since as many as 50 photoreceptor genes must be expressed at high levels to maintain survival (55, 56).

Murine rod photoreceptors also maintain a highly specialized inverted nuclear organization in which euchromatin is located adjacent to the nuclear lamina and heterochromatin is greatly expanded and centralized (6, 7, 57, 58). Intriguingly, *Crx* and *Nrl* are also essential for establishing higher-order chromosome-looping configurations in both rods and cones (59), and mutants exhibit macroscopic nuclear disorganization in rods (60–63). While these transcription factors thus control higher-order genome organization, it seems unlikely that they act directly to control the striking reorganization (7) and expansion (57, 58) of heterochromatin observed during rod maturation, since both are prominently associated with euchromatin. Our data suggest instead that *Cas21* contributes to heterochromatin organization and expansion in rod photoreceptors (Fig. 8 *L–N*).

***Cas21* Safeguards Rod Gene Expression.** While a previous study had concluded that *Cas21* protein was localized within the cytoplasm of photoreceptors (24), we suggest that this finding failed to take into account the unusual nuclear organization of rod photoreceptors. Examination of *Cas21* immunohistochemistry using Airyscan confocal microscopy allowed us to resolve *Cas21* localization below the Rayleigh diffraction limit, which revealed clear nuclear staining. Moreover, we showed independently that *Cas21* protein was associated with transcriptional modifiers such as the polycomb repressor complex and that these cofactors were essential for *Cas21*-dependent functions. Finally, transcriptome analysis of *Cas21*-cKO cells confirms that rod gene expression is reduced as early as P2 (*SI Appendix*, Fig. S1), which likely contributes to the eventual photoreceptor degeneration observed in old retinas. *Cas21* was localized to the euchromatin of rods and cones but is prominently localized to the margins of chromocenters in retinal progenitors (21) or in transfected 3T3 fibroblasts. Further experiments will be required to understand what regulates this shift in nuclear localization.

Lamin A Is Sufficient to Reorganize and Reposition the Rod Photoreceptor Nucleus. To understand the effects of *Cas21* on the rod photoreceptor nucleus, we examined known determinants of the nuclear lamina. We initially focused on *Lbr*, since it was the only determinant previously shown to be sufficient to reverse rod chromatin inversion (8). To our surprise, we observed no obvious effect of *Cas21* on *Lbr* expression in rods; moreover, we found that weak *Lbr* expression persisted in adult stages. Indeed, the latter observation was recently reported by Hughes et al. (64), who performed genomic and transcriptomic analysis of sorted rods and cones. They suggested instead that lamin A/C might be the critical determinant of rod chromatin inversion, since the *Lmna* gene is completely silent and becomes inaccessible in differentiated rods. Our reanalysis of published RNA-seq data and our own expression profiling (*SI Appendix*, Fig. S5) confirm that *Lbr* levels fall in accordance with Solovei et al. (8), at the level of both transcript and protein, and that these levels never reach zero, in accordance with Hughes et al. (64). We submit that the very low levels of *Lbr* expressed by adult rods likely fall below a functional threshold.

The clear up-regulation of lamin A/C in both *Cas21*-KO and polycomb RNAi was nevertheless perplexing, as lamin C had

previously been shown to have no effect on chromatin inversion (8). Moreover, it had been suggested that lamin A is not expressed in neurons (65). However, when examining published RNA-seq data (66, 67), we observed that lamin A was quantitatively the dominant transcript in cone photoreceptors (*SI Appendix*, Fig. S5). Accordingly, when we expressed lamin A in rods, we found that it was sufficient to reorganize rod chromatin architecture and reposition the nucleus to the apical side of the photoreceptor layer. That these activities are specific to lamin A and not lamin C is in agreement with human mutations associated with Hutchinson–Guilford progeria syndrome, which abolish the splicing and processing of the lamin A C terminus and concomitantly abrogate heterochromatin tethering (68–70).

While the mechanistic basis for effects on nuclear position remains to be clarified, we note that the apical localization of cone photoreceptors requires linkers of the nucleoskeleton to the cytoskeleton (LINC) proteins (37–39, 41, 42), suggesting that in rods lamin A/C might provide an anchor for the LINC proteins, allowing them to transmit forces to the nucleus.

While *Cas21* regulates the nuclear organization of rods, its role in cone photoreceptors remains to be determined. We hypothesize that *Cas21* might also be required for cone nuclear organization, but the more conventional nuclear architecture of cones is not as simple to analyze using microscopy. Moreover, lamin A/C remains expressed in cones, albeit at low levels, whereas it is undetected in rods. It is therefore possible that *Cas21*/polycomb simply reduces lamin A/C expression levels in cones. Another possibility is that rod- and cone-specific transcription factors alter the function of *Cas21*. Rod-specific polycomb complexes have recently been shown to repress cone gene expression (71), suggesting that *Cas21* might conversely function to suppress rod-specific genes in cones. Importantly, we carefully examined rods manipulated via *Cas21* cKO or polycomb RNAi to confirm that lamin A/C up-regulation and nuclear reorganization occur independently of a rod vs. cone fate switch (*SI Appendix*, Fig. S3).

Degeneration, lamin A/C up-regulation, and nuclear reorganization appear to be a slow process in *Cas21*-KO retinas, whereas these processes appeared much faster when using RNAi to knockdown *Cas21* or polycomb. We suggest that this is probably due to the slow kinetics of Cre-mediated exon excision, as both Cre drivers lead to mosaic recombination. Indeed, we observe many “escaper” cells in the retinas of *Rod-cKO* mutants as late as P300. RNAi manipulations may also lead to lamin A/C up-regulation before rod maturation, whereas the *LMOP::Cre* driver, which is active only from P7 onward (29, 72), may lead to *Cas21* inactivation after rods have completed chromatin inversion. Preventing chromatin inversion might thus be more efficient than reversing it.

Cooperation Between *Cas21v2* and Polycomb in Regulating Rod Lamina Function. We had previously shown that only the *Cas21v2* isoform promotes rod production when misexpressed in retinal progenitors (21). Intriguingly, we find that *Cas21v2*, but not *Cas21v1*, associates with polycomb proteins, suggesting a mechanistic basis for the functional differences elicited by the two splice forms. However, this finding is difficult to explain at the structural level, since the amino acid sequence of *Cas21v2* is completely represented within the longer *Cas21v1* transcript, except for the single amino acid residue at the C terminus of *Cas21v2*. One possibility is that the longer C-terminal domain of *Cas21v1* sterically hinders the interaction with Rnf2.

Polycomb recruitment to the genome is a mysterious and poorly understood subject, and much work remains to be done before concluding that *Cas21* regulates this process directly. However, our functional data strongly suggest that *Cas21* and polycomb cooperate to regulate the function of the nuclear lamina, acting to suppress the expression of lamin A/C. Accordingly,

rods mutant for the polycomb gene *Bmi1* have been shown to exhibit heterochromatin decondensation (73), which closely resembles the phenotype we found in *Cas1*-KO rods, and polycomb marks are observed on the *Lmna* promoter and gene body in rod-specific ChIP-seq datasets (*SI Appendix, Fig. S5*) (67). Like *Bmi1*, *Cas1* associates with polycomb repressive complex 1 (PRC1), which has numerous variants. Interestingly, *Samd7*, another PRC1-associated protein, was recently shown to suppress cone gene expression in rod photoreceptors (71). Although lamin A/C is expressed in cones and not rods, we do not see up-regulation of other cone markers in *Cas1*-cKO rods (*SI Appendix, Fig. S3*) or in our RNA-seq dataset. Moreover, both *Cas1* and other polycomb mutants degenerate (73–75), whereas *Samd7* mutants do not. These data suggest the existence of multiple PRC1 variants with nonoverlapping functions.

Whether alterations in lamina function can explain the cell death observed here in *Cas1* Rod-cKO mutants and in retinal polycomb mutants (73, 75, 76), the exact molecular mechanism remains to be formally determined. We note, however, that lamin A expression alters the nuclear organization of rods at the macroscopic level. Disorganized nuclear organization was previously shown to lead to defective partitioning of euchromatic genes into heterochromatin in degenerating *Sca7* transgenic rods (61), where lamin A/C is also up-regulated (8). Additionally, murine rods normally maintain their euchromatic transcriptional apparatus at the nuclear periphery and perhaps at the nuclear lamina itself (77). We hypothesize that the conversion of this territory to a suppressive transcriptional environment by lamin A disrupts photoreceptor gene expression, as supported by our RNA-seq analysis of *Cas1*-cKO retinas. This hypothesis is countered by results from *Lbr* transgenic mice, which do not appear to degenerate, suggesting that nuclear reorganization and degeneration are separable (8). However, it remains unclear whether the nuclear reorganization triggered by *Lbr* versus lamin A/C is equivalent. Indeed, *Lbr* is expressed naturally in rods, whereas lamin A/C is never normally expressed (*SI Appendix, Fig. S5*). More work will be required to determine whether and how gene expression and nuclear organization are linked in *Cas1*-KO rods.

Our results suggest that *Cas1* and lamina proteins contribute oppositely to chromatin inversion and that the specific outcome observed depends on protein dosage. For example, overexpressing *Cas1v2* led to the precocious inversion and expansion of heterochromatin, both in *Lbr*⁺ retinal progenitors and immature rods. *Cas1v2* misexpression similarly promoted the basal localization of *Lbr*⁺ rod photoreceptor nuclei in transfected explants. Moreover, overexpressing *Cas1* in *Lbr*⁺ retinal progenitors or lamin A/C⁺ 3T3 fibroblasts likewise led to the expansion and/or aggregation of chromocenters. These data suggest that *Cas1* can bypass the effects of lamina tethers to promote aspects of chromatin inversion. On the other hand, overexpression of lamin A reduced heterochromatin area in *Cas1*⁺ rod photoreceptors and blocked the ability of *Cas1* to localize rod nuclei to the basal side of the photoreceptor layer, even when *Cas1* was cotransfected. Finally, heterochromatin is maintained in normal configuration in retinal progenitor cells, which express both *Cas1* (21) and *Lbr* (8). We suggest that the increasing expression levels of *Cas1v2* observed during retinal development (21) progressively contribute to chromatin inversion. In the future, it will be of interest to define how exactly *Cas1* and lamin A/C expression are opposed at the posttranscriptional level.

In conclusion, this study uncovers *Cas1* as a regulator of nuclear architecture essential for cell survival. Since *Cas1* is expressed in other types of neurons as well as tissues such as muscle and skin (21–23), we propose that it might function similarly to control nuclear organization in many different cell types.

Methods

A detailed description of the materials and methods is presented in *SI Appendix, Methods*.

Animal Care. All animal work was performed in accordance with guidelines from the Institut de Recherches Cliniques de Montréal (IRCM) animal care committee and the Canadian Council on Animal Care. CD1 mice were obtained from Taconic. *Cas1*^{Flox/Flox} (21), *α-Pax6::Cre* (46), *LMOP::Cre* (72), *IKCre-A* (78), and *R26-Stop-EYFP* (79) alleles and genotyping protocols were previously described. (See also *SI Appendix, Methods and Table S1*.) No differences were observed between Cre[−] and Cre⁺ heterozygote animals, which therefore are referred to as “control” throughout the text and figures. Animals of either sex were used.

Biochemistry. Immunoprecipitation and Western blotting from cultured cell lines were performed as described previously, with minor modifications (29). Cross-linking-assisted immunoprecipitation was performed as described (33). Antibodies and concentrations are presented in *SI Appendix, Methods and Table S2*.

Histology. In vivo and ex vivo retinal transfection, tissue fixation, and immunohistochemistry were performed essentially as described (21, 29). Antibodies and concentrations are presented in *SI Appendix, Methods and Table S2*. For TEM, 1-y-old animals were perfused with fixative composed of 2.5% glutaraldehyde, 2% paraformaldehyde in 100 mM cacodylate buffer (pH 7.0), and 2 mM CaCl₂. Retinal tissue was passed through an acetone dehydration buffer series, sectioned to 90–100 nm, and imaged using an FEI Tecnai 12 BioTwin instrument. Further details are presented in *SI Appendix, Methods*.

Quantitation and Statistical Analysis. Statistical operations were conducted using Microsoft Excel and GraphPad Prism 6 software. To measure nuclear position, the photoreceptor layer of transfected retinal regions was divided into equal-sized bins, each covering 25% of the layer. The nuclear position of transfected cells was then marked, and the proportions of nuclei in each bin were quantitated. To measure heterochromatin and euchromatin areas, regions of the nucleus were traced manually in TEM images or confocal z-planes using the Freehand Selection Tool in the ImageJ (NIH) software package. Measured areas were related to the total area of the nucleus. The *n* values refer to independent experiments or animals as per the text.

RNA-Seq Analysis. RNA-seq methods and bioinformatics are described in *SI Appendix, Methods*. Data have been deposited in the GEO database (accession no. GSE115778).

ACKNOWLEDGMENTS. We thank Irina Solovei for generously sharing reagents and advice; Harald Herrmann and Monika Zwerger for antibodies; Cheryl Arrowsmith, Harohiko Koseki, Heinrich Leonhardt, and Bas Van Steensel for sharing DNA constructs; Christine Jolicoeur for invaluable technical support; Jessica Barthe and Marie-Claude Lavallée for animal husbandry; Julie Lord and Éric Massicote for help with flow cytometry; Odile Neyret-Djossou and Alexis Blanchet-Cohen for help with RNA-seq experiments; and members of the M.C. laboratory and the IRCM Neuroscience laboratories for insightful discussions. This work was supported by the Foundation for Fighting Blindness Canada and the Canadian Institutes of Health Research (CIHR) Operating Grant PJT-148553. P.M. was supported by a CIHR postdoctoral fellowship and currently holds the Gladys and Lorna J. Wood Chair for Research in Vision. M.C. holds the Gaëtan and Roland Pillenière Chair in Retina Biology and is a Research Scholar Emeritus of the Fonds de Recherche du Québec-Santé.

1. Misteli T (2008) Physiological importance of RNA and protein mobility in the cell nucleus. *Histochem Cell Biol* 129:5–11.
2. Monier K, Armas JC, Etteldorf S, Ghazal P, Sullivan KF (2000) Annexation of the interchromosomal space during viral infection. *Nat Cell Biol* 2:661–665.
3. Lieberman-Aiden E, et al. (2009) Comprehensive mapping of long-range interactions reveals folding principles of the human genome. *Science* 326:289–293.
4. Rao SS, et al. (2014) A 3D map of the human genome at kilobase resolution reveals principles of chromatin looping. *Cell* 159:1665–1680.

5. Dixon JR, et al. (2012) Topological domains in mammalian genomes identified by analysis of chromatin interactions. *Nature* 485:376–380.
6. Eberhart A, et al. (2013) Epigenetics of eu- and heterochromatin in inverted and conventional nuclei from mouse retina. *Chromosome Res* 21:535–554.
7. Solovei I, et al. (2009) Nuclear architecture of rod photoreceptor cells adapts to vision in mammalian evolution. *Cell* 137:356–368.
8. Solovei I, et al. (2013) LBR and lamin A/C sequentially tether peripheral heterochromatin and inversely regulate differentiation. *Cell* 152:584–598.

9. Charpentier MS, et al. (2013) CASZ1 promotes vascular assembly and morphogenesis through the direct regulation of an EGLF/RhoA-mediated pathway. *Dev Cell* 25:132–143.
10. Christine KS, Conlon FL (2008) Vertebrate CASTOR is required for differentiation of cardiac precursor cells at the ventral midline. *Dev Cell* 14:616–623.
11. Liu Z, et al. (2014) Essential role of the zinc finger transcription factor Casz1 for mammalian cardiac morphogenesis and development. *J Biol Chem* 289:29801–29816.
12. Cui X, Doe CQ (1992) ming is expressed in neuroblast sublineages and regulates gene expression in the Drosophila central nervous system. *Development* 116:943–952.
13. Mellerick DM, Kassiss JA, Zhang SD, Odenwald WF (1992) Castor encodes a novel zinc finger protein required for the development of a subset of CNS neurons in Drosophila. *Neuron* 9:789–803.
14. Vacalla CM, Theil T (2002) Cst, a novel mouse gene related to Drosophila castor, exhibits dynamic expression patterns during neurogenesis and heart development. *Mech Dev* 118:265–268.
15. Baumgardt M, Karlsson D, Terriente J, Diaz-Benjumea FJ, Thor S (2009) Neuronal subtype specification within a lineage by opposing temporal feed-forward loops. *Cell* 139:969–982.
16. Grosskortenhaus R, Robinson KJ, Doe CQ (2006) Pdm and castor specify late-born motor neuron identity in the NB7-1 lineage. *Genes Dev* 20:2618–2627.
17. Kambadur R, et al. (1998) Regulation of POU genes by castor and hunchback establishes layered compartments in the Drosophila CNS. *Genes Dev* 12:246–260.
18. Maurange C, Cheng L, Gould AP (2008) Temporal transcription factors and their targets schedule the end of neural proliferation in Drosophila. *Cell* 133:891–902.
19. Tran KD, Doe CQ (2008) Pdm and castor close successive temporal identity windows in the NB3-1 lineage. *Development* 135:3491–3499.
20. Stampfel G, et al. (2015) Transcriptional regulators form diverse groups with context-dependent regulatory functions. *Nature* 528:147–151.
21. Mattar P, Ericson J, Blackshaw S, Cayouette M (2015) A conserved regulatory logic controls temporal identity in mouse neural progenitors. *Neuron* 85:497–504.
22. Amin NM, Gibbs D, Conlon FL (2014) Differential regulation of CASZ1 protein expression during cardiac and skeletal muscle development. *Dev Dyn* 243:948–956.
23. Blackshaw S, et al. (2004) Genomic analysis of mouse retinal development. *PLoS Biol* 2:E247.
24. Liu Z, et al. (2017) Identification of CASZ1 NES reveals potential mechanisms for loss of CASZ1 tumor suppressor activity in neuroblastoma. *Oncogene* 36:97–109.
25. Omori Y, et al. (2011) Analysis of transcriptional regulatory pathways of photoreceptor genes by expression profiling of the Otx2-deficient retina. *PLoS One* 6:e19685.
26. Samuel A, Housset M, Fant B, Lamonerie T (2014) Otx2 ChIP-seq reveals unique and redundant functions in the mature mouse retina. *PLoS One* 9:e89110.
27. Le YZ, et al. (2004) Targeted expression of Cre recombinase to cone photoreceptors in transgenic mice. *Mol Vis* 10:1011–1018.
28. Skarnes WC, et al. (2011) A conditional knockout resource for the genome-wide study of mouse gene function. *Nature* 474:337–342.
29. Ramamurthy V, et al. (2014) Numb regulates the polarized delivery of cyclic nucleotide-gated ion channels in rod photoreceptor cilia. *J Neurosci* 34:13976–13987.
30. Cayouette M, Behn D, Sendtner M, Lachapelle P, Gravel C (1998) Intracellular gene transfer of ciliary neurotrophic factor prevents death and increases responsiveness of rod photoreceptors in the retinal degeneration slow mouse. *J Neurosci* 18:9282–9293.
31. Cayouette M, Smith SB, Becerra SP, Gravel C (1999) Pigment epithelium-derived factor delays the death of photoreceptors in mouse models of inherited retinal degenerations. *Neurobiol Dis* 6:523–532.
32. Zhang J, et al. (2013) SFMBT1 functions with LSD1 to regulate expression of canonical histone genes and chromatin-related factors. *Genes Dev* 27:749–766.
33. Mohammed H, et al. (2016) Rapid immunoprecipitation mass spectrometry of endogenous proteins (RIME) for analysis of chromatin complexes. *Nat Protoc* 11:316–326.
34. Liu Z, Lam N, Thiele CJ (2015) Zinc finger transcription factor CASZ1 interacts with histones, DNA repair proteins and recruits NuRD complex to regulate gene transcription. *Oncotarget* 6:27628–27640.
35. Morimoto-Suzuki N, et al. (2014) The polycomb component Ring1B regulates the timed termination of subcortical projection neuron production during mouse neocortical development. *Development* 141:4343–4353.
36. Tardat M, et al. (2015) Cbx2 targets PRC1 to constitutive heterochromatin in mouse zygotes in a parent-of-origin-dependent manner. *Mol Cell* 58:157–171.
37. Insinna C, Baye LM, Amsterdam A, Beshare JC, Link BA (2010) Analysis of a zebrafish dync1h1 mutant reveals multiple functions for cytoplasmic dynein 1 during retinal photoreceptor development. *Neural Dev* 5:12.
38. Maddox DM, et al. (2015) A mutation in Syne2 causes early retinal defects in photoreceptors, secondary neurons, and Müller glia. *Invest Ophthalmol Vis Sci* 56:3776–3787.
39. Razafsky D, Blecher N, Markov A, Stewart-Hutchinson PJ, Hodzic D (2012) LINC complexes mediate the positioning of cone photoreceptor nuclei in mouse retina. *PLoS One* 7:e47180.
40. Razafsky D, et al. (2016) Lamin B1 and lamin B2 are long-lived proteins with distinct functions in retinal development. *Mol Biol Cell* 27:1928–1937.
41. Tsujikawa M, Omori Y, Biyanwila J, Malicki J (2007) Mechanism of positioning the cell nucleus in vertebrate photoreceptors. *Proc Natl Acad Sci USA* 104:14819–14824.
42. Yu J, et al. (2011) KASH protein Syne2/nesprin-2 and SUN proteins SUN1/2 mediate nuclear migration during mammalian retinal development. *Hum Mol Genet* 20:1061–1073.
43. de Melo J, Peng GH, Chen S, Blackshaw S (2011) The Spalt family transcription factor Sal3 regulates the development of cone photoreceptors and retinal horizontal interneurons. *Development* 138:2325–2336.
44. Emerson MM, Surzenko N, Goetz JJ, Trimarchi J, Cepko CL (2013) Otx2 and Onecut1 promote the fates of cone photoreceptors and horizontal cells and repress rod photoreceptors. *Dev Cell* 26:59–72.
45. Nijnik A, et al.; Sanger Institute Microarray Facility; Sanger Mouse Genetics Project (2012) The critical role of histone H2A-deubiquitinase Mym1 in hematopoiesis and lymphocyte differentiation. *Blood* 119:1370–1379.
46. Marquardt T, et al. (2001) Pax6 is required for the multipotent state of retinal progenitor cells. *Cell* 105:43–55.
47. Razafsky DS, Ward CL, Kolb T, Hodzic D (2013) Developmental regulation of linkers of the nucleoskeleton to the cytoskeleton during mouse postnatal retinogenesis. *Nucleus* 4:399–409.
48. Wong-Riley MT (2010) Energy metabolism of the visual system. *Eye Brain* 2:99–116.
49. Andzelm MM, et al. (2015) MEF2D drives photoreceptor development through a genome-wide competition for tissue-specific enhancers. *Neuron* 86:247–263.
50. Béby F, et al. (2010) Otx2 gene deletion in adult mouse retina induces rapid RPE dystrophy and slow photoreceptor degeneration. *PLoS One* 5:e11673.
51. Freund CL, et al. (1997) Cone-rod dystrophy due to mutations in a novel photoreceptor-specific homeobox gene (CRX) essential for maintenance of the photoreceptor. *Cell* 91:543–553.
52. Koike C, et al. (2007) Functional roles of Otx2 transcription factor in postnatal mouse retinal development. *Mol Cell Biol* 27:8318–8329.
53. Morrow EM, Furukawa T, Lee JE, Cepko CL (1999) NeuroD regulates multiple functions in the developing neural retina in rodent. *Development* 126:23–36.
54. Omori Y, et al. (2015) Mef2d is essential for the maturation and integrity of retinal photoreceptor and bipolar cells. *Genes Cells* 20:408–426.
55. Hsiao TH, et al. (2007) The cis-regulatory logic of the mammalian photoreceptor transcriptional network. *PLoS One* 2:e643.
56. Siebert S, et al. (2009) Genetic address book for retinal cell types. *Nat Neurosci* 12:1197–1204.
57. Kizilyaprak C, Spehner D, Devys D, Schultz P (2010) In vivo chromatin organization of mouse rod photoreceptors correlates with histone modifications. *PLoS One* 5:e11039.
58. Popova EY, et al. (2013) Developmentally regulated linker histone H1c promotes heterochromatin condensation and mediates structural integrity of rod photoreceptors in mouse retina. *J Biol Chem* 288:17895–17907.
59. Peng GH, Chen S (2011) Active opsin loci adopt intrachromosomal loops that depend on the photoreceptor transcription factor network. *Proc Natl Acad Sci USA* 108:17821–17826.
60. Corbo JC, Cepko CL (2005) A hybrid photoreceptor expressing both rod and cone genes in a mouse model of enhanced S-cone syndrome. *PLoS Genet* 1:e11.
61. Helminger D, et al. (2006) Glutamine-expanded ataxin-7 alters TFTC/STAGA recruitment and chromatin structure leading to photoreceptor dysfunction. *PLoS Biol* 4:e67.
62. Hennig AK, Peng GH, Chen S (2013) Transcription coactivators p300 and CBP are necessary for photoreceptor-specific chromatin organization and gene expression. *PLoS One* 8:e69721.
63. Tran NM, et al. (2014) Mechanistically distinct mouse models for CRX-associated retinopathy. *PLoS Genet* 10:e1004111.
64. Hughes AE, Enright JM, Myers CA, Shen SQ, Corbo JC (2017) Cell type-specific epigenomic analysis reveals a uniquely closed chromatin architecture in mouse rod photoreceptors. *Sci Rep* 7:43184.
65. Jung HJ, et al. (2012) Regulation of prelamin A but not lamin C by miR-9, a brain-specific microRNA. *Proc Natl Acad Sci USA* 109:E423–E431.
66. Kim JW, et al. (2016) Recruitment of rod photoreceptors from short-wavelength-sensitive cones during the evolution of nocturnal vision in mammals. *Dev Cell* 37:520–532.
67. Mo A, et al. (2016) Epigenomic landscapes of retinal rods and cones. *eLife* 5:e11613.
68. Goldman RD, et al. (2004) Accumulation of mutant lamin A causes progressive changes in nuclear architecture in Hutchinson-Gilford progeria syndrome. *Proc Natl Acad Sci USA* 101:8963–8968.
69. McCord RP, et al. (2013) Correlated alterations in genome organization, histone methylation, and DNA-lamin A/C interactions in Hutchinson-Gilford progeria syndrome. *Genome Res* 23:260–269.
70. Shumaker DK, et al. (2006) Mutant nuclear lamin A leads to progressive alterations of epigenetic control in premature aging. *Proc Natl Acad Sci USA* 103:8703–8708.
71. Omori Y, et al. (2017) Samd7 is a cell type-specific PRC1 component essential for establishing retinal rod photoreceptor identity. *Proc Natl Acad Sci USA* 114:E8264–E8273.
72. Le YZ, et al. (2006) Mouse opsin promoter-directed Cre recombinase expression in transgenic mice. *Mol Vis* 12:389–398.
73. Barabino A, et al. (2016) Loss of Bmi1 causes anomalies in retinal development and degeneration of cone photoreceptors. *Development* 143:1571–1584.
74. Iida A, et al. (2015) Roles of histone H3K27 trimethylase Ezh2 in retinal proliferation and differentiation. *Dev Neurobiol* 75:947–960.
75. Yan N, et al. (2016) Postnatal onset of retinal degeneration by loss of embryonic Ezh2 repression of Six1. *Sci Rep* 6:33887.
76. Ueno K, et al. (2016) Transition of differential histone H3 methylation in photoreceptors and other retinal cells during retinal differentiation. *Sci Rep* 6:29264.
77. Wang X, et al. (2002) Barrier to autointegration factor interacts with the cone-rod homeobox and represses its transactivation function. *J Biol Chem* 277:43288–43300.
78. Tarchini B, Jolicoeur C, Cayouette M (2012) In vivo evidence for unbiased Ikaros retinal lineages using an Ikaros-Cre mouse line driving clonal recombination. *Dev Dyn* 241:1973–1985.
79. Srinivas S, et al. (2001) Cre reporter strains produced by targeted insertion of EYFP and ECFP into the ROSA26 locus. *BMC Dev Biol* 1:4.